TECHNICAL REPORT 2060
December 2014

Underwater Source-Level Estimation using Sparsity-Cognizant Source-Location Mapping

Logan Straatemeier
Paul A. Baxley
Pedro A. Forero

SSC Pacific
San Diego, CA 92152-5001

SSC Pacific
San Diego, California 92152-5001

K. J. Rothenhaus, CAPT, USN
Commanding Officer

C. A. Keeney
Executive Director

ADMINISTRATIVE INFORMATION

The work described in this report was performed by the IO Spectrum Exploitation Branch (Code 56140) and the Advanced Research Branch (Code 56490), Space and Naval Warfare Systems Center Pacific (SSC Pacific), San Diego, CA. The Naval Innovative Science and Engineering (NISE) Program at SSC Pacific funded this team effort as a Basic Research project.

Released by
R. W. Krafton, Head
IO Spectrum Exploitation Branch

Under authority of
G. Settelmayer. Head
Information Operations
Division

SB

EXECUTIVE SUMMARY

In this work, we present a method to estimate the acoustic source gain of targets in a shallow-water environment, using passive sonar. This is accomplished by using a two-step approach. The first step is to localize the target, which is accomplished by using the Sparsity-Cognizant Source Location Mapping (scSLM) algorithm, developed at the Space and Naval Warfare Systems Center Pacific. This algorithm has been shown to be robust to environmental mismatch when localizing multiple targets. Moreover, it yields an estimate of the source levels. Unfortunately, the bias in these estimates can be large depending on the values of the algorithm's tuning parameters. The second step of our approach is introduced to decrease the bias in the acoustic source gain estimates. By using the locations obtained by scSLM and the environmental model, we develop an estimator that yields improved acoustic source gain estimates. Numerical tests are used to illustrate the quality of the acoustic source gain estimates for multiple broadband targets in a shallow-water environment.

CONTENTS

Figures

1. INTRODUCTION

Localization of an underwater target and then estimation of its acoustic gain using passive sonar is a difficult task. Localization and estimation in shallow-water scenarios is particularly challenging due to the complexities of acoustic propagation through this environment. For low-frequency signals, acoustic propagation in shallow water is characterized by multipath due to the multiple interactions that they sustain with the sea surface and sea floor, by refraction due to a depth-dependent sound speed profile, and by the spatio-temporal variability of environmental parameters. Shipping lanes and marine life also contribute noise that masks/interferes with the acoustic signals of interest and leads to low signal-to-noise ratios (SNRs) at the hydrophone array [1].

Various matched-field processing (MFP) algorithms are useful in localization of underwater acoustic sources. MFP assumes that sources are located in a predefined area and uses an acoustic propagation model to predict the pressure fields, known as replicas, at the hydrophone array for a grid of locations. These replicas are then "matched" to the hydrophone measurements to produce an ambiguity surface, which summarizes the acoustic power estimates across the grid. Then localization is achieved by choosing the largest peaks on the ambiguity surface and assigning them to source locations. Classical MFP suffers from large sidelobes, which makes localization of multiple sources difficult and can be sensitive to environmental mismatch [2].

Different from MFP, Sparsity-Cognizant Source Location Mapping (scSLM) casts the localization problem as a group-Lasso regression problem. It has been shown that location estimates obtained via scSLM are more accurate than the ones obtained by classical MFP algorithms, such as Bartlett and Capon [3]. It has also been shown that they are robust to environmental mismatch [3]. This work uses the scSLM algorithm to localize the targets and estimate their acoustic gain. It is then shown that the acoustic source gain estimates provided by the scSLM's output do not accurately estimate the true source gain. A two-step approach, using scSLM for the localization and a least-squares estimator for obtaining the source gains yields improved source gain estimates. This method differs from ones found in literature, that tend to use a simplified passive wave equation to estimate the acoustic source-levels of ships and marine life [4–6]. One of the main problems with using a simplified passive wave equation in a shallow-water environment is the fact that it does not account for multipath or spatio-temporal variability of environmental parameters.

$Notation$: upper (lower) boldface letters are used for matrices (column vectors);$(\cdot)$'$((\cdot)^{\dagger})$ denotes matrix and vector transpose (conjugate transpose);$[\cdot]_{n,m}([\cdot]_n)$ the (n,m)-entry of a matrix (n-entry of a vector); $\|\mathbf{y}\|_q = \left(\sum_{n=1}^{N} |y_n|^q\right)^{1/q}$

2. PROBLEM FORMULATION

An array of *N* hydrophones with known and arbitrary geometry is used to capture *T* discrete-time acoustic measurements $\{y(t)\}_{t=1}^{T}$ from K sources. Let $y_n(t) := [y(t)]_n$ correspond to the acoustic measurements gathered by the n-th hydrophone at time t. With $h_n(t; \mathbf{r}_k)$ being the discrete-time impulse response of the channel at time t and unknown source location $\mathbf{r}_k \in \mathbb{R}^d$, where $d \in \{2, 3\}$, $y_n(t)$ is modeled as

$$y_n(t) = \sum_{k=1}^{K} \left(h_n * s_k\right)(t; \mathbf{r}_k) + \epsilon_n(t), \qquad n = 1, ..., N \tag{1}$$

where $*$ denotes the convolution operator, $s_k(t)$ the acoustic signature for the k-th source and $\epsilon_n(t)$ is a zero-mean random measurement noise.

Although it is possible to work directly in the time domain, the computational complexity required to do so, can be excessive [7]. Instead, the problem is cast in the frequency domain. First, $\{y(t)\}_{t=1}^{T}$ is partitioned into M blocks and transformed to the frequency domain via the discrete Fourier transform (DFT). Per frequency w_f, let $\mathbf{y}_{m,f} \in \mathbb{C}^{\mathbb{N}}$ and $s_{k,f} \in \mathbb{C}$ denote the DFT coefficient vector for the m-th measurement block and the acoustic gain DFT coefficient for the n-th source, respectively. Then, $\{\mathbf{y}_{m,f}\}_{m=1}^{M}$ is modeled as

$$\mathbf{y}_{m,f} = \sum_{k=1}^{K} s_{k,f}\left(\mathbf{p}_{k,f} + \mathbf{v}_{k,f}\right) + \epsilon_{m,f}, \qquad m = 1, ..., M \tag{2}$$

where $\epsilon_{m,f}$ denotes the Fourier coefficients at w_f corresponding to the noise in the m-th block; $\mathbf{p}_{k,f} \in \mathbb{C}^N$ the w_f model-predicted Fourier coefficients at the array for a source located at $\mathbf{r}_k$, which will be referred to as replicas; and $\mathbf{v}_{k,f} \in \mathbb{C}^N$ an unknown perturbation vector effecting $\mathbf{p}_{k,f}$, which helps account for the mismatch between the acoustic propagation model and the true propagation environment.

Let $\mathbf{Y}_f := [\mathbf{y}_{1,f}, ..., \mathbf{y}_{M,f}]$ comprise all M Fourier coefficients vectors at w_f. Given an underwater propagation model, Fourier coefficients $\{\mathbf{Y}_f\}_{f=1}^{F}$ for F frequencies $\{w_f\}_{f=1}^{F}$ and the number of sources K. The localization process seeks to find the positions $\{\mathbf{r}_k\}_{k=1}^{K}$ while still being robust to unknown perturbations $\{\{\mathbf{v}_{k,f}\}_{k=1}^{K}\}_{f=1}^{F}$. Even if the adopted underwater propagation model were to exactly characterize the propagation environment, solving for $\{\mathbf{r}_k\}_{k=1}^{K}$ is difficult because it entails a nonlinear regression problem. A closed-form expression relating $\mathbf{r}_k$ to $\mathbf{p}_{k,f}$ is unavailable since in most cases of interest, finding $\mathbf{p}_{k,f}$ entails solving the wave equation for specific boundary conditions given by the environment model [1].

2.1 LOCALIZATION

The scSLM algorithm circumvents some of the computational challenges posed by the nonlinear relationship between $\mathbf{r}_k$ and $\{\mathbf{p}_{k,f}\}_{f=1}^{F}$, by constructing a grid $\mathcal{G} := \left\{\mathbf{r}_g \in \mathbb{R}^d\right\}_{g=1}^{G}$ that spans the region of interest. Let $\mathbf{p}_{g,f}$ denote the replica vector at frequency w_f for a source located at $\mathbf{r}_g$. For a given w_f, $\mathbf{P}_f := [\mathbf{p}_{1,f}, ..., \mathbf{p}_{G,f}] \in \mathbb{C}^{N \times G}$ comprises all normalized replicas corresponding to $\mathcal{G}$ where $\|\mathbf{p}_{g,f}\|_2 = 1, \forall g$. Each $\mathbf{y}_{m,f}$ is now modeled as

$$\mathbf{y}_{m,f} = \sum_{g=1}^{G} s_{g,f}(\mathbf{p}_{g,f} + \mathbf{v}_{g,f}) + \epsilon_{m,f}, \qquad \forall m, f \tag{3}$$

where $\mathbf{v}_{g,f} \in \mathbb{C}^N$ denotes the unknown perturbation vector affecting $\mathbf{p}_{g,f}$. Since K $\ll$ G, most of the $\{s_{g,f}\}$'s are expected to be zero.

Let $\mathbf{s}_f := [s_{1,f}, ..., s_{G,f}]' \in \mathbb{C}^G$ denote the complex-valued vector of regression coefficients at w_f, $\mathbf{S} := [\mathbf{s}_1, ..., \mathbf{s}_F] \in \mathbb{C}^{G\times F}$ denote the complex-valued matrix comprising all regression coefficients, $\mathbf{V}_f := [\mathbf{v}_{1,f}, ..., \mathbf{v}_{G,F}] \in \mathbb{C}^{N\times G}$ a complex-valued matrix comprising all perturbation vectors. The scSLM algorithm uses an ℓ_1/ℓ_q regularizer, also known as a group-Lasso regularizer, to find the optimal $\mathbf{S}$ while being robust to environmental mismatch. Equation 3 can be cast as a convex optimization problem that forces sparsity and coherence, in the source locations across frequencies, see [8, 9] for a detailed description. In this work coherence refers to a common support across source localization maps at different frequencies, which is reasonable to exploit since it is assumed the source locations are immutable across frequencies. The scSLM algorithm solves the following minimization problem:

$$\min_{\mathbf{S}\in\mathbb{C}^{G\times F}} \frac{1}{2M}\sum_{f=1}^{F}\mathbb{E}\left\|\mathbf{Y}_f - (\mathbf{P}_f + \mathbf{V}_f)\,\mathbf{s}_f 1_M^{'}\right\|^2 + \mu\sum_{g=1}^{G}\|\varsigma_g\|_q \tag{4}$$

where ς_g is defined as the g-th row vector of $\mathbf{S}$, $\varsigma_g := [s_{g,1}, ..., s_{g,F}]$. $\mu > 0$ is a tuning parameter controlling the sparsity level on $\mathbf{S}$ and $q \in (1, \infty]$. The scSLM algorithm assumes that the columns of $\mathbf{V}_f$ are zero-mean random vectors with covariance matrix $\mathbf{\Sigma}_f \in \mathbb{C}^{G\times G}$ and independent across $\mathbf{V}_f$'s.

By choosing μ, one can construct a map with K nonzero locations that correspond to the source locations [10].

2.2 SOURCE LEVEL ESTIMATION

One should note that Equation (4) gives both an estimate of the source location and the acoustic gains. However, since $s_{g,f}$ was calculated using normalized replicas the estimate does not correspond to the true acoustic gain, but rather it corresponds to the acoustic source gain decreased by the acoustic propagation loss from the source to array. To compute the source gain estimate, we need to remove the normalization of the replica that was used to obtain $s_{g,f}$. Letting $\{g_k^*\}_{k=1}^K$ be the grid points that correspond to the K top ranked intensities from the scSLM algorithm, we obtain the following acoustic gain estimates

$$\hat{s}_{g_k^*,f} = \frac{s_{g_k^*,f}}{\left\|\mathbf{p}_{g_k^*,f}\right\|_2}. \tag{5}$$

One caveat with this method of estimating the source level, $\hat{s}_{g_k^*,f}$ is that it yields biased estimates since it is based on the group-Lasso regularizer [8].

To circumvent this problem, we propose to use the estimated location of the source g_k^*, but will then use the least-squares estimator to find the source gains. Since the scSLM algorithm guarantees a common support and each frequency has an independent source level, we can obtain the source gains for each frequency separately. Letting $\mathbf{P}_f^K := [\mathbf{p}_{g_1^*,f}, ..., \mathbf{p}_{g_K^*,f}]$ and $\mathbf{s}_f^K := [s_{g_1^*,f}, ..., s_{g_K^*,f}]'$, we postulate the following estimator for the source levels, $\tilde{s}_f^K$:

$$\tilde{\mathbf{s}}_f^K := \underset{\mathbf{s}_f^K\in\mathbb{C}^{K\times 1}}{\arg\min} \left\|\mathbf{y}_f - \mathbf{P}_f^K\mathbf{s}_f^K\right\|_2^2, \tag{6}$$

which has the following closed form solution:

$$\tilde{\mathbf{s}}_f = \left(\mathbf{P}_f^{K\dagger}\mathbf{P}_f^K\right)^{-1}\left(\mathbf{P}_f^{K\dagger}\right)\mathbf{y}_f. \tag{7}$$

Note that if there is only one source present, Equation (7) simplifies to the following form:

$$\tilde{\mathbf{s}}_f = \frac{\mathbf{p}_{g_1^*,f}{}^{\dagger}\mathbf{y}_f}{\left\|\mathbf{p}_{g_1^*,f}\right\|_2^2}. \tag{8}$$

3. NUMERICAL TESTS

This section serves to illustrate the estimation quality of the acoustic source gains in a broadband multi-source environment, using passive sonar. Numerical tests on synthetic data sets were conducted to illustrate the performance of the proposed algorithm.

A shallow-water environment, as depicted in Figure 1a, was created. This environment contains a vertical line hydrophone array, which consists of $N = 25$ elements that span the entire water column of 100 m. A grid of 10,251 locations spanning a range 0 to 10 km and depths 0 to 100 m was used. This gives a range and depth spacing of 50 and 2 m, respectively. All replicas for this environment were calculated using KRAKEN [11].

We first consider a single broadband source and the following five frequencies: 65, 150, 220, 300, and 350 Hz. These five frequencies correspond to the following source gains: 95, 97, 100, 97, and 95 dB, respectively (Figure 1b). We then introduce additive white Gaussian noise to the replicas to obtain a predefined average SNR across the frequencies. The average SNR was calculated at the closest point of approach (CPA) and will vary according to the targets distance (Figure 2).

Next we simulate a two source case. Both sources are emitting at the same five frequencies and same acoustic gains: 65, 150, 220, 300, and 350 Hz, and 95, 97, 100, 97, and 95 dB, respectively. The difference in the two sources are the CPA and depth values as can be seen in Figure 3.

For all tests, we considered a correct localization to be a square of ± 1 around the true location, as shown in Figure 4. We also do not allow multiple targets to localize within the same area of localization. For the following tests, scSLM with $q = 2$ was used.

3.1 RESULTS

The following results show the average estimates over 50 Monte Carlo runs. scSLM parameters α and λ were set to 0.005 and 0.85 respectively.

3.1.1 ONE SOURCE

For the single source case, the average SNR at CPA was set to 3 dB. The resulting SNR's per frequency is shown in Figure 2. Figure 6 shows that the scSLM acoustic source gain estimations are not an accurate portrayal of the true signal strengths. Again, this is due to the innate bias of scSLM, that stems from its reliance on the group-Lasso regularizer. Since this bias occurs in all the scSLM source level estimations, we will no longer show these results. When first localizing the sources based on scSLM and then using the least-squares estimator from Equation (6) to estimate the source levels, we are able to better approximate the true acoustic gain (Figure 7). Note that as the SNR drops, localization becomes more difficult. Hence, estimating the source acoustic gains also becomes more difficult. This is shown in the larger error-bars in Figures 6 and 7.

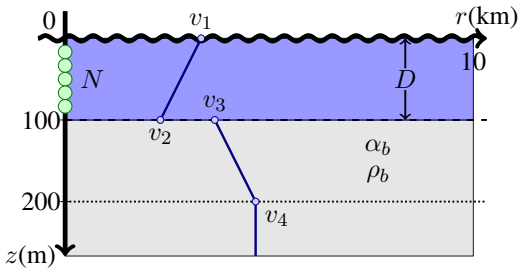

(a) Environment

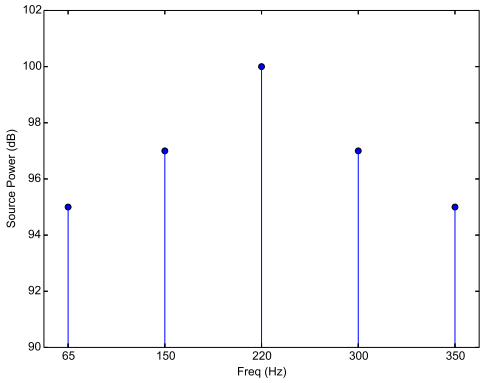

(b) Signal power

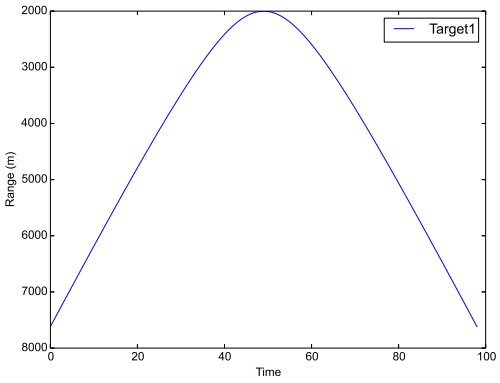

(c) True source - Range

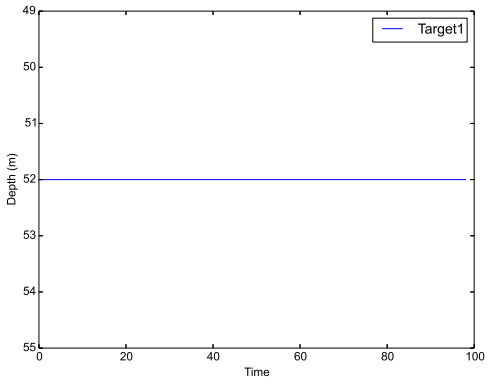

(d) True source - Depth

Figure 1. Simulation setup - Schematic of the underwater acoustic propagation model used for the simulation. Sample parameter values for this acoustic propagation model are $v_1 = 1,500$ m/s, $v_2 = 1,460$ m/s, $v_3 = 1,600$ m/s, $v_4 = 1,750$ m/s, $v_5 = 1,750$ m/s, $\alpha_b = 0.2$ dB/m/KHz, and $\rho_b = 1.8$ g/cm^3.

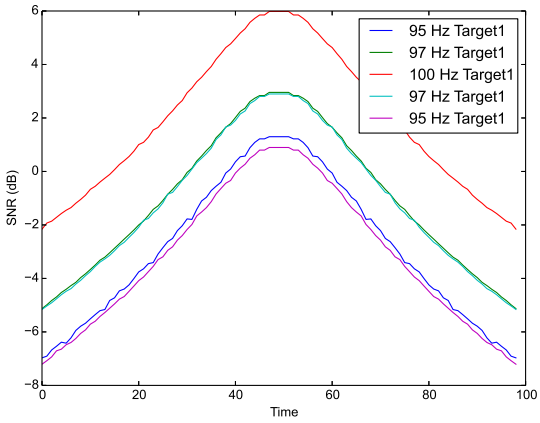

Figure 2. SNR of each frequency - one source.

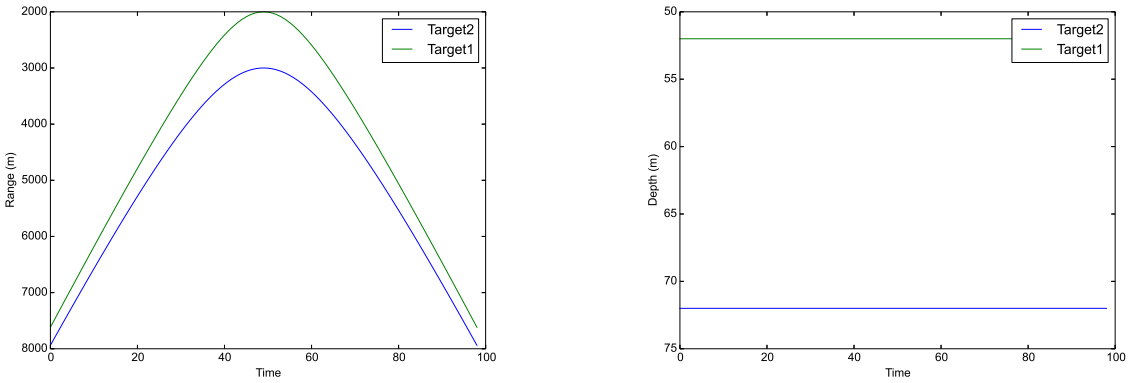

(a) True source - Range (b) True source - Depth

Figure 3. Simulated range and depth of the two sources.

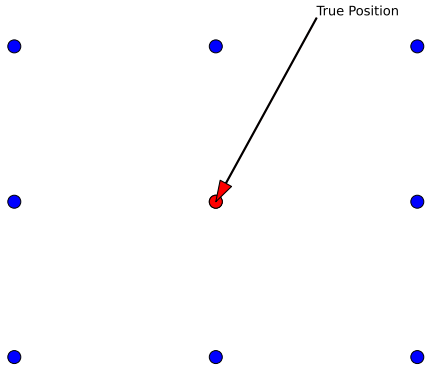

Figure 4. Correct localization region.

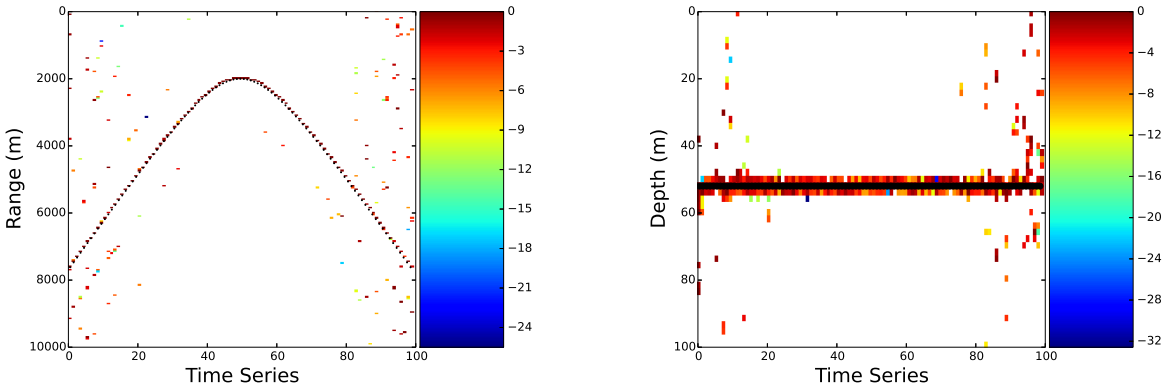

(a) Range (b) Depth

Figure 5. Location estimates from scSLM for a single source.

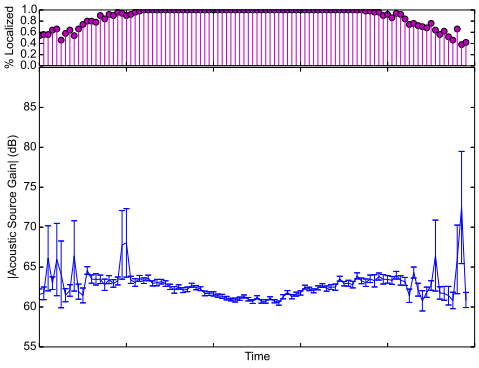

(a) Frequency = 65 Hz

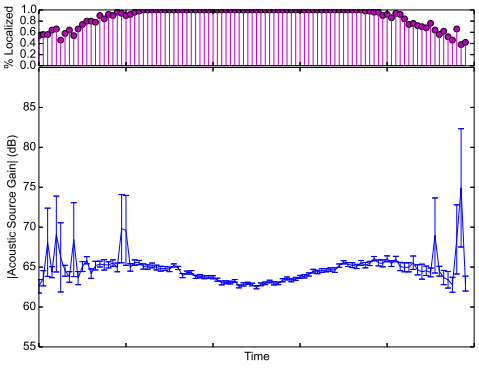

(b) Frequency = 150 Hz

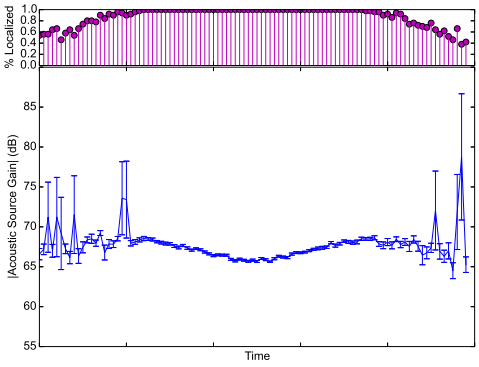

(c) Frequency = 220 Hz

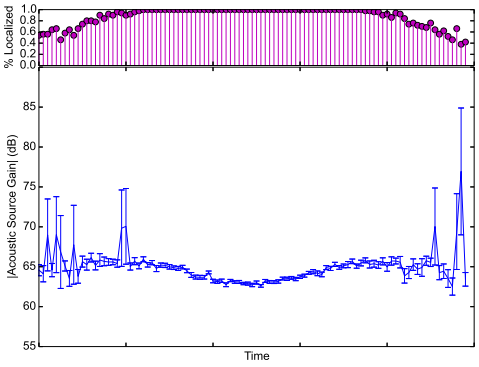

(d) Frequency = 300 Hz

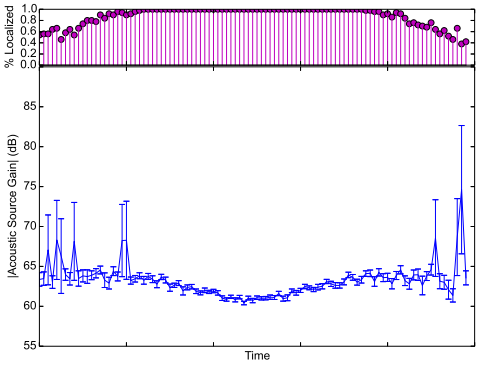

(e) Frequency = 350 Hz

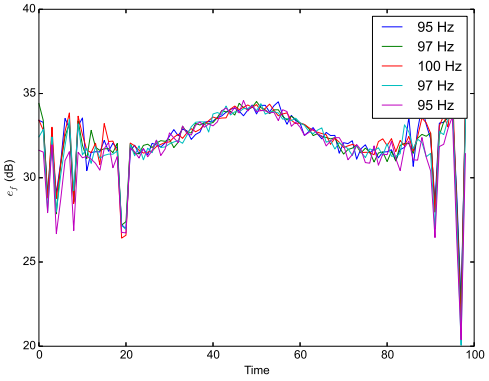

(f) Average error

Figure 6. Single Source: Acoustic source gain estimates obtained via scSLM. The stem plots represent the percentage of correct localizations estimated via 50 Monte Carlo runs. The source gain plot shows the average gain magnitude in dB, $20\,log_{10}(|\,\bar{\hat{s}}_f|)$, along with its standard deviation. The average error plot corresponds to $e_f = 20\,log_{10}(\big||s_f| - |\,\bar{\hat{s}}_f|\big|)$. The true source gain, at frequency f, and the average source gain from the Monte Carlo runs is $s_f, \bar{\hat{s}_f}$, respectively.

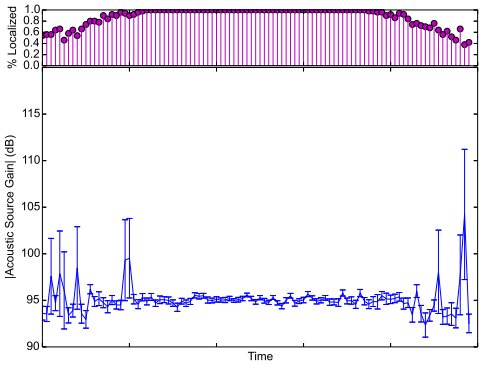

(a) Frequency = 65 Hz

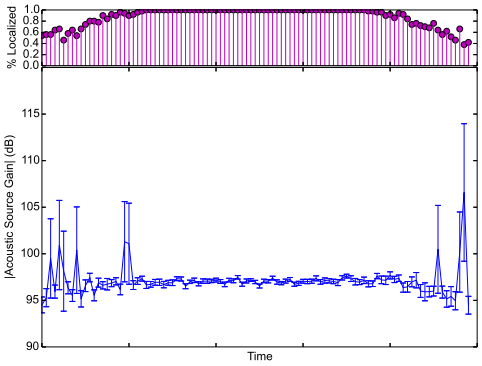

(b) Frequency = 150 Hz

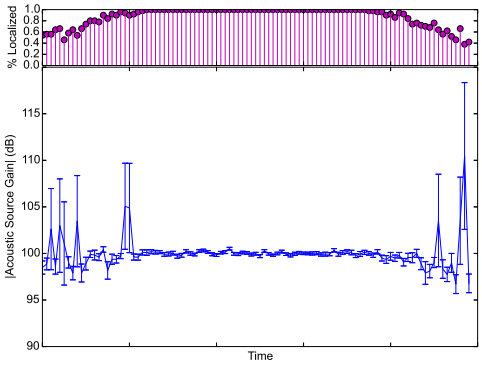

(c) Frequency = 220 Hz

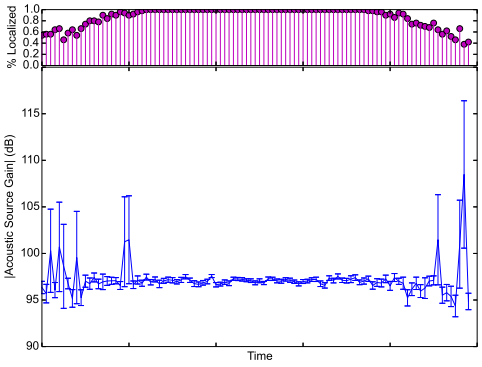

(d) Frequency = 300 Hz

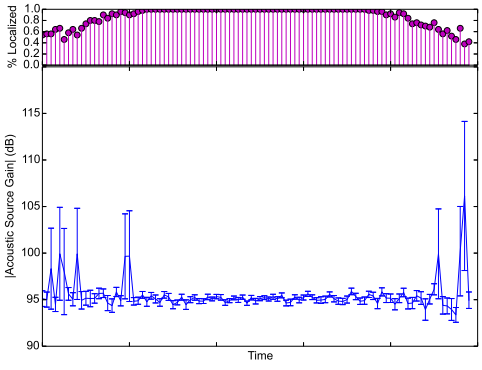

(e) Frequency = 350 Hz

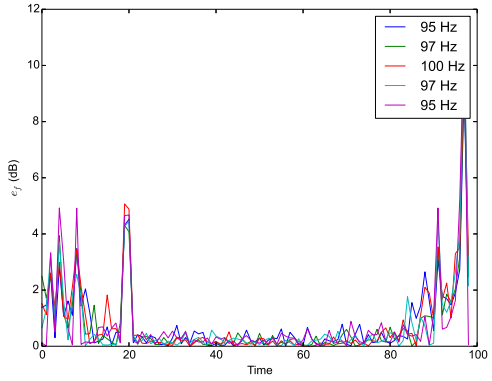

(f) Average error

Figure 7. Single Source: Acoustic source gain estimates obtained via least-squares. The stem plots represent the percentage of correct localizations estimated via 50 Monte Carlo runs. The source gain plot shows the average gain magnitude in dB, $20\,log_{10}(|\,\bar{\tilde{s}}_f|)$, along with its standard deviation. The average error plot corresponds to $e_f = 20\,log_{10}(\big||s_f| - |\,\bar{\tilde{s}}_f|\big|)$. The true source gain, at frequency f, and the average source gain from the Monte Carlo runs is $s_f, \bar{\tilde{s}}_f$, respectively.

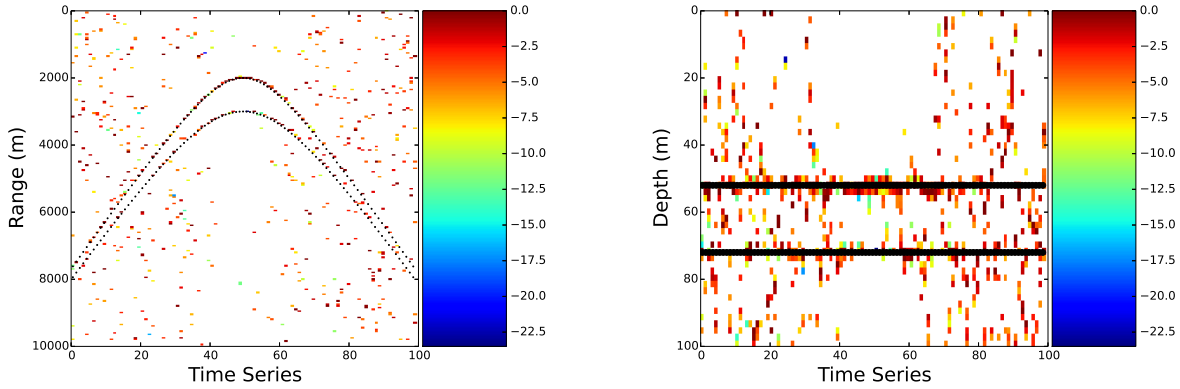

Figure 8. Location estimates for two sources.

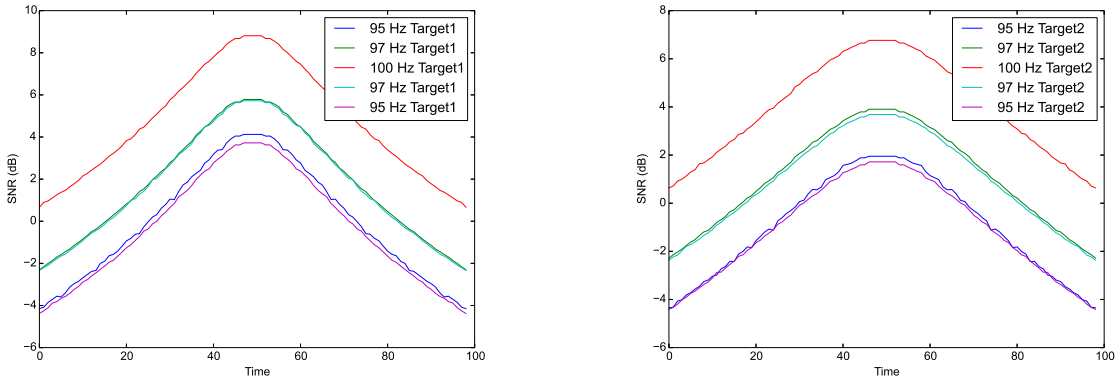

Figure 9. SNR for each target.

3.1.2 TWO SOURCES

In the two-source simulation, we increased the average SNR at CPA to 8 dB (Figure 9). Target 1 will be defined as the source at the depth of 52 m, while target 2 will be the source at 72 m (Figure 3). The results of the two-source Monte Carlo simulation are shown in Figures 10 and 11. These figures illustrate that correct localizations on multiple targets can be difficult, even at higher SNRs (compared with the single-source case). These figures also show that target 1 was localized more often than target 2 and that the error-bars on target 1 at each frequency do not vary as much as target 2. The smaller variations are likely caused by the incorrect localization providing fallacious source gain estimates. As the targets approach CPA, the acoustic gains were closer to the expected values, along with having lower variances. This is most likely due to the increase in localization percentages and higher SNRs.

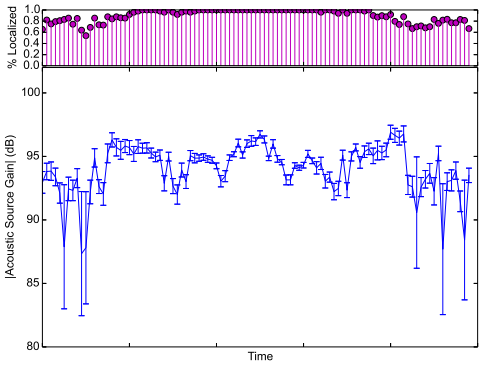

(a) Frequency = 65 Hz

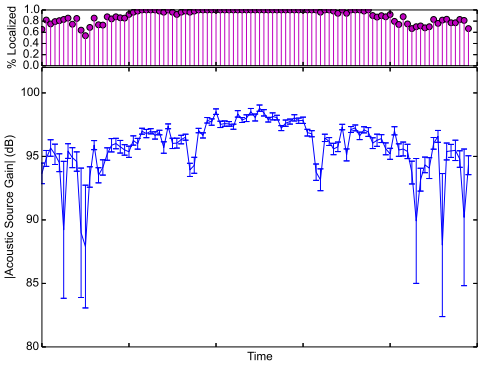

(b) Frequency = 150 Hz

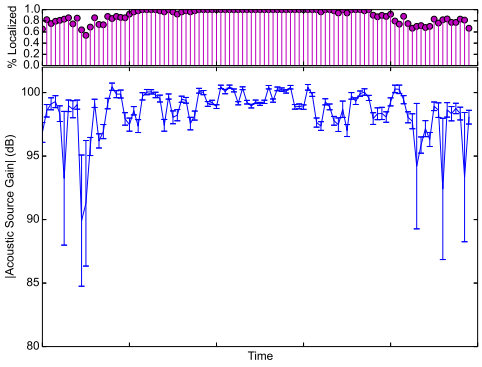

(c) Frequency = 220 Hz

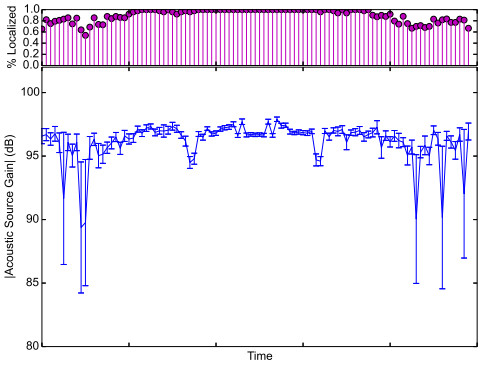

(d) Frequency = 300 Hz

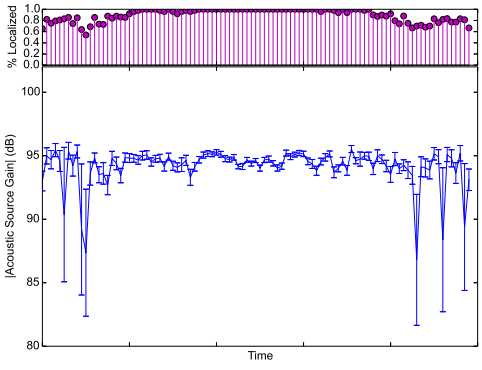

(e) Frequency = 350 Hz

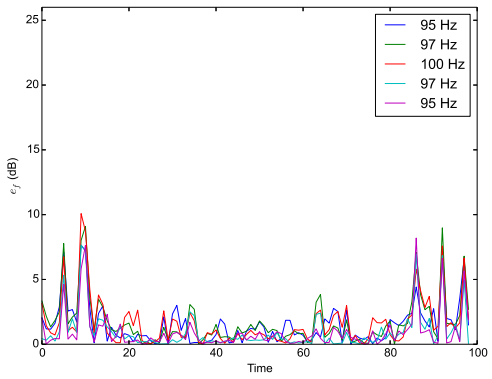

(f) Average error

Figure 10. Two Sources: Target 1 acoustic source gain estimates obtained via least-squares. The stem plots represent the percentage of correct localizations estimated via 50 Monte Carlo runs. The source gain plot shows the average gain magnitude in dB, $20\,log_{10}(|\,\tilde{\bar{s}}_f|)$, along with its standard deviation. The average error plot corresponds to $e_f = 20\,log_{10}(\big||s_f| - |\,\tilde{\bar{s}}_f|\big|)$. The true source gain, at frequency f, and the average source gain from the Monte Carlo runs is $s_f, \tilde{\bar{s}}_f$, respectively.

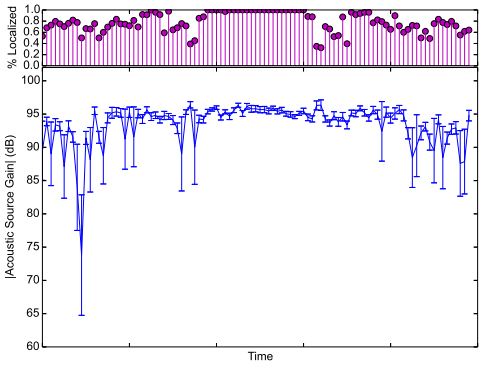

(a) Frequency = 65 Hz

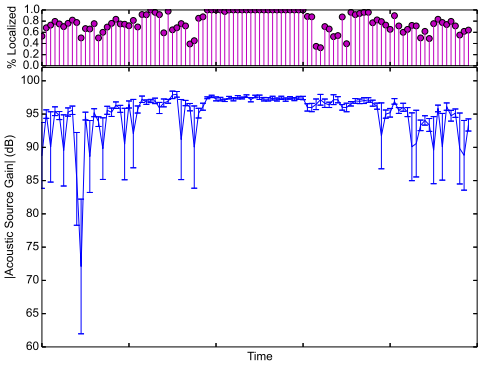

(b) Frequency = 150 Hz

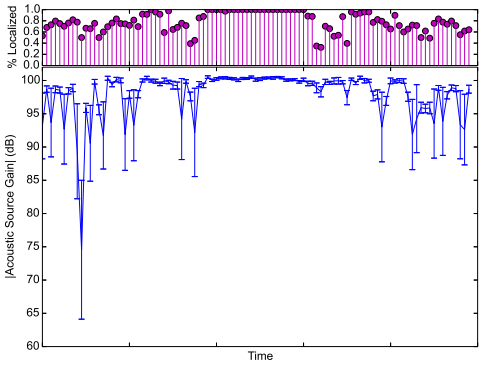

(c) Frequency = 220 Hz

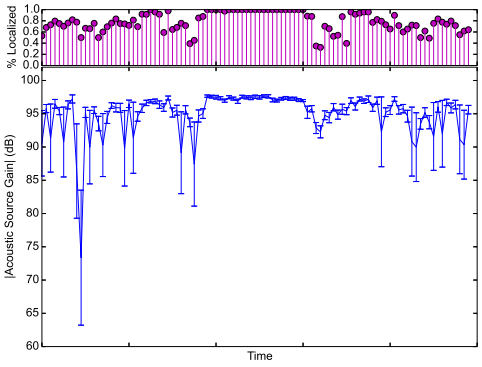

(d) Frequency = 300 Hz

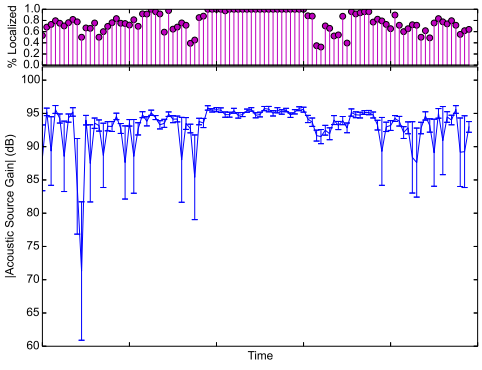

(e) Frequency = 350 Hz

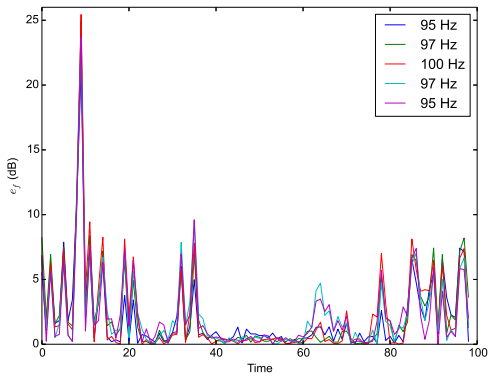

(f) Average error

Figure 11. Two Sources: Target 2 acoustic source gain estimates obtained via least-squares. The stem plots represent the percentage of correct localizations estimated via 50 Monte Carlo runs. The source gain plot shows the average gain magnitude in dB, $20\,log_{10}(|\,\bar{\tilde{s}}_f|)$, along with its standard deviation. The average error plot corresponds to $e_f = 20\,log_{10}(\big||s_f| - |\,\bar{\tilde{s}}_f|\big|)$. The true source gain, at frequency f, and the average source gain from the Monte Carlo runs is $s_f, \bar{\tilde{s}}_f$, respectively.

4. CONCLUSIONS

This work focused on estimating the acoustic source gains of broadband sources in a shallow-water environment. The results show that accurate acoustic source gain estimation is possible if the sources were correctly localized. Knowledge about the environment was a fundamental enabler for the acoustic source gain estimation. When dealing with multiple sources the source gain estimation does not perform as well, but if localization was achieved, then it is still able to give accurate results at higher SNRs. Future research will explore how this algorithm performs on real data set(s) and in the presence of environmental uncertainty.

REFERENCES

1. Jensen, F. B., Kuperman, W. A., Porter, M. B., and H.Schmidt. 2011. *Computational Ocean Acoustics*, 2 ed. Springer, New York, NY.

2. Porter, M. B. and Tolstoy, A. 1994. "The Matched Field Processing Benchmark Problems," *Journal of Computational Acoustics*, vol. 02, no. 03, pp. 161–185.

3. Forero, P. A. and Baxley, P. 2014. "Shallow-Water Sparsity-Cognizant Source-Location Mapping," *Journal of Acoustic Society of America*, vol. 135, pp. 3483–3501.

4. Trevorrow, M. V., Vasiliev, B., and Vagle, S. May 2008. "Directionality and Maneuvering Effects on Surface Ship Underwater Acoustic Signature," *Journal of Acoustic Society of America*, vol. 124, pp. 767–778.

5. Gedamke, J., Costa, D. P., and Dunstan, A. 2001. "Localization and Visual Verification of Complex Minke Whale Vocalization," *Journal of Acoustic Society of America*, vol. 109, pp. 3038–3047.

6. Borowski, B., Sutin, A., Roh, H. S., and Bunin, B. 2008. "Passive Acoustic Threat Detection in Estuarin Environments." *Proc. SPIE 6945, Optics and Photonics in Global Homeland Security IV*, April 15, Orlando, FL.

7. Czenszak, S. and Krolik, J. 1997. "Robust Wideband Matched-field Processing with a Short Vertical Array," *Journal of Acoustic Society of America*, vol. 101, no. 2, pp. 749–759.

8. Simon, N., Friedman, J., Hastie, T., and Tibshirani, R. 2013. "A Sparse-Group Lasso," *Journal of Computational Graphical Statistics*, vol. 22, no. 2, pp. 231–245.

9. Hastie, T., Tibshirani, R., and Friedman, J. 2009. *The Elements of Statistical Learning: Data Mining, Inference, and Prediction*, 2nd ed. Springer, New York, NY.

10. Forero, P. A. 2014. "Broadband Underwater Source Localization via Multitask Learning," *Information Sciences and Systems (CISS)*, March 19-21, Princeton, NJ.

11. Porter, M. 1991. "The Kraken Normal Mode Program," Tech. rep., SACLANT Undersea research Center Memorandum (SM-245) and Naval Research Laboratory Mem. Report 6920.

REPORT DOCUMENTATION PAGE

Form Approved
OMB No. 0704-01-0188

D

PLEASE DO NOT RETURN YOUR FORM TO THE ABOVE ADDRESS.

1. REPORT DATE *(DD-MM-YYYY)*	**2. REPORT TYPE**	**3. DATES COVERED** *(From - To)*
December 2014	Final	

4. TITLE AND SUBTITLE

Underwater Source Level Estimation using Sparsity-Cognizant Source-Location Mapping

5a. CONTRACT NUMBER

5b. GRANT NUMBER

5c. PROGRAM ELEMENT NUMBER

6. AUTHORS

Logan Straatemeier
Paul A. Baxley
Pedro A. Forero

5d. PROJECT NUMBER

5e. TASK NUMBER

5f. WORK UNIT NUMBER

7. PERFORMING ORGANIZATION NAME(S) AND ADDRESS(ES)

SSC Pacific, 53560 Hull Street, San Diego, CA 92152–5001

8. PERFORMING ORGANIZATION REPORT NUMBER

TR 2060

9. SPONSORING/MONITORING AGENCY NAME(S) AND ADDRESS(ES)

Naval Innovative Science and Engineering (NISE) Program (Basic Research)
SSC Pacific, 53560 Hull Street, San Diego, CA 92152–5001

10. SPONSOR/MONITOR'S ACRONYM(S)

11. SPONSOR/MONITOR'S REPORT NUMBER(S)

12. DISTRIBUTION/AVAILABILITY STATEMENT

Approved for public release.

13. SUPPLEMENTARY NOTES

14. ABSTRACT

This work focused on estimating the acoustic source gains of broadband sources in a shallow-water environment. The results show that accurate acoustic source gain estimation is possible if the sources were correctly localized. Knowledge about the environment was a fundamental enabler for the acoustic source gain estimation. When dealing with multiple sources, the source gain estimation does not perform as well, but if localization was achieved, then it is still able to give accurate results at higher signal-to-noise ratios. Future research will explore how this algorithm performs on real data set(s) and in the presence of environmental uncertainty.

15. SUBJECT TERMS

Mission Area:
localization source level estimation matched-field processing algorithms sparsity-cognizant source location mapping

16. SECURITY CLASSIFICATION OF:			**17. LIMITATION OF ABSTRACT**	**18. NUMBER OF PAGES**	**19a. NAME OF RESPONSIBLE PERSON**
a. REPORT	**b. ABSTRACT**	**c. THIS PAGE**			Logan Straatemeier
U	U	U	U	21	**19B. TELEPHONE NUMBER** *(Include area code)* (619) 553-2020

INITIAL DISTRIBUTION

84300	Library	(2)
85300	Archive/Stock	(1)
56140	L. Straatemeier	(1)
56490	P. A. Baxley	(1)
56490	P. A. Forero	(1)

Defense Technical Information Center
Fort Belvoir, VA 22060–6218 (1)

Approved for public release.

SSC Pacific
San Diego, CA 92152-5001